Microwave Tomography Using DBIM with Double Mesh Scheme

Latifah Mohamed
School of Electrical Systems Engineering
Universiti Malaysia Perlis
Arau, Malaysia
latifah@unimap.edu.my

Yoshihiko Kuwahara
Graduate School of Integrated Science and Technology
Shizuoka University
Hamamatsu, Japan
tykuwab@ipc.shizuoka.ac.jp

***Abstract*— It is necessary to assure the accuracy of forward calculation with high resolution to acquire accurate image reconstruction. For the forward calculation to be accurate, a fine mesh is used which will accurately determine the electric field everywhere in imaging region. However, due to limited number of measurements can be achieved for any realistic lab-scale system, a coarse mesh with less unknown parameters is required to avoid limited illness and thus can reduce the calculation cost in inverse problem. In this paper, a double mesh scheme in image reconstruction stage is introduced to detect small objects while decreasing calculation cost and assuring the accuracy of the forward calculation.**

Keywords—microwave tomography; breast cancer detection; DBIM; double mesh

I. INTRODUCTION

In Japan, the breast cancer incidence and mortality rates of women are lower compared to the United States and the European Union. Still, it is one of the leading causes of death among women and shows tendency to increase every year [1]. Therefore, an early breast cancer detection is crucial because it can be expected to cure completely by early treatment. Recently, early breast cancer detection by microwave imaging has attracted much interest among researchers. The dielectric properties contrast between the constituent breast tissues offers the physical basis for microwave imaging [2]. We are currently considering the development of microwave tomography for reconstructing the dielectric properties of breast [3]-[5].

In the previous report in [3], we confirmed the image reconstruction by solving the inverse problem using the Newton-Kantorovich procedure in [6]. In this method, since an extensive calculation of inverse matrix is carried out to compute the Jacobian, there were problems such as low resolution and high computational cost. Therefore, in this paper we employ distorted Born iterative method (DBIM) to reconstruct the dielectric properties distribution. This method does not require inverse matrix calculation in the Jacobian computation as described in [7][8].

It is necessary to assure accuracy of the forward calculation with high resolution to achieve accurate image reconstruction [9]. For forward calculation, a fine mesh is used which will accurately determine the electric field in imaging region [10]. However, since the limited number of measurements can be achieved for any realistic lab-scale system, a coarse mesh with less unknown parameters is required to avoid illposeness and thus can reduce the calculation cost in inverse problem [11].

In this paper, a double mesh scheme in image reconstruction stage is introduced to detect small objects while decreasing calculation cost and assuring the accuracy of the forward calculation.

II. METHODOLOGY

A. Inverse Scattering Problem and DBIM

In tomography, an imaging object is discretized and expressed as a group of voxels. The total number of voxels in the imaging area is N, and the dielectric contrast is represented by κ. The calculated data Y_{mn} obtained by the antenna array based on the estimated contrast are compared with the measured data X_{mn} by the actual model (m = 1, ..., N, n = 1, ..., N, N is the total number of antennas, m subscript is the number of transmitter, n subscript is the number of receiver). The contrast of modeled breast is iteratively estimated and updated by Gauss-Newton method until $X_{mn} = Y_{mn}$ is reached. Practically, the image reconstruction is

accomplished by minimizing the norm of the difference between measured and calculated scattering data.

In this report, we consider an inhomogeneous medium with finite volume V enclosing unknown parameters which is discretized and characterized by contrast κ. This volume V is embedded in homogeneous background permittivity ε^b. The contrast function is given by (1) to model the human breast tissue.

$$\kappa = \sigma + j\omega\varepsilon_o\left(\varepsilon_r - \varepsilon^b\right) \tag{1}$$

where σ is conductivity, ε_o is permittivity of free space, and ε_r is relative permittivity. The contrast of each unknown parameters (σ, ε_r) within volume V is defined as a $K \times 1$ vector. The volume V is illuminated by L transmitters in sequence, and the scattering field from the object at an observation location **r** is formulated as

$$\mathbf{E}^s(\mathbf{r}) = \omega^2\mu\int_V \overline{G}^b(\mathbf{r}\,|\,\mathbf{r}')\mathbf{E}^t(\mathbf{r}')\left[\kappa(\mathbf{r}') - \kappa^b(\mathbf{r}')\right]d\mathbf{r}' \tag{2}$$

where **r'** is arbitrarily position vector in imaging region V, ω is angular frequency, μ is magnetic permeability, and scattering field $\mathbf{E}^S$ is the difference between the field observed in the object and the field observed in the background. This scattering field is determined by Green's function G^b, total field $\mathbf{E}^t$, and the dielectric contrast function κ. In our algorithm, the total field is calculated by method of moment [6].

Equation (2) is a nonlinear integral equation, therefore we employ DBIM to linearize the equation. In (2), $\mathbf{E}^t$ in V is approximated by the background field $\mathbf{E}^b$, which is calculated iteratively based on the estimated current contrast. Equation (1) is applied to (2) and discretized, thus resulting a linear relationship between the scattered field and contrast function. Since the two unknown parameters are real numbers, the equation is divided into the real and imaginary part to form linear equations of real number as expressed in (3).

$$\begin{bmatrix} \Re\left\{\frac{\partial\kappa}{\partial\sigma}\mathbf{B}\right\} & \Re\left\{\frac{\partial\kappa}{\partial\varepsilon_r}\mathbf{B}\right\} \\ \Im\left\{\frac{\partial\kappa}{\partial\sigma}\mathbf{B}\right\} & \Im\left\{\frac{\partial\kappa}{\partial\varepsilon_r}\mathbf{B}\right\} \end{bmatrix}\begin{bmatrix}\Delta\sigma \\ \Delta\varepsilon_r\end{bmatrix} = \begin{bmatrix}\Re\{\mathbf{E}^s\} \\ \Im\{\mathbf{E}^s\}\end{bmatrix} \tag{3}$$

$$\mathbf{B} = \omega^2\mu\varepsilon_o\overline{G}^b(\mathbf{r}\,|\,\mathbf{r}')\mathbf{E}^t(\mathbf{r}\,|\,\mathbf{r}')$$

$$\Delta\sigma = \sigma - \sigma^b \qquad \Delta\varepsilon_r = \varepsilon_r - \varepsilon_r^b$$

where $\Re\{\ \}$ and $\Im\{\ \}$ denotes the real and imaginary part of the complex number, respectively. $\mathbf{E}^S$ is the difference between the calculated scattered field and the measured scattered field. The system in (3) can be denoted as a linear system equation $\mathbf{Ax} = \mathbf{b}$.

In DBIM, it begins with an initial guess for the background contrast. In the linear model of (3), the contrast perturbations $\mathbf{x} = (\sigma, \varepsilon_r)$ is determined by (4).

$$\mathbf{x} = \left(A^T A\right)^{-1} A^T\mathbf{b} \tag{4}$$

Since the inversion in (4) is ill-posed, Tikhonov regularization is applied at each iteration and estimates the contrast perturbations in finite volume V. Then the contrast is updated and used as the background contrast to recalculate the revised background field and scattered field. This process repeated until the residual norm of scattering field is smaller to the set criteria.

B. Image Reconstruction with Double Mesh Scheme

In our image reconstruction, double mesh scheme is used to increase the resolution image of a designated portion and to decrease the calculation cost in the inverse problem. The double mesh scheme utilizes two meshes, where a fine mesh in forward problem defines the forward solutions x_f, and both of course mesh and fine mesh in inverse problem determines the unknown parameters x_c to be reconstructed [12]. The distribution of forward solution x_f and unknown parameters x_c are reconstructed iteratively. These parameters come and go between two kinds of meshes in each iteration as shown in the flow chart in Fig. 1.

III. RESULTS AND DISCUSSION

A. Analysis Model

In this study, we used an imaging sensor with dimension of 9.6 cm x 4.8 cm x 9.6 cm comprised of 4 planar arrays with 6 antennas installed on each side wall, and 12 antennas on the top. These antennas are embedded in the dielectric properties which has almost the same value of adipose (fatty) tissue. The antennas shown in Fig. 2 are arranged to generate vertical and horizontal polarized incident field. Among the antennas, one

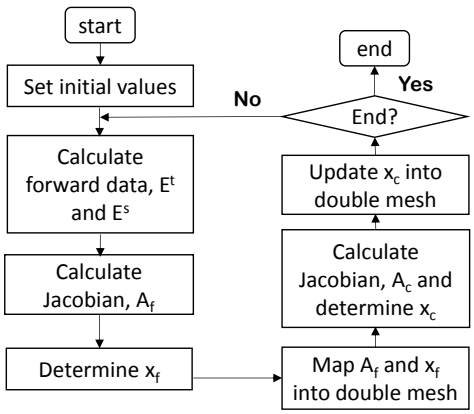

Fig. 1. Flow chart of double mesh reconstruction algorithm

antenna is used for transmitting, and all the elements including transmitter are used for receiving data. The dot lines in the imaging sensor represent the polarization direction of the antenna, with y-axis indicates a vertical direction. This imaging area is discretized to 2601 cubic cells to produce 6 mm resolution, and characterized with complex permittivity of background, in the form of {ε, σ} = {6.2, 0.15 [S/m]}.

For our study, a simple breast is modeled in Fig. 3 by a hemisphere with radius of 4.8 cm. It consists of adipose tissue, fibro-glandular tissue and a tumor (radius 4 mm). We assumed that the boundary of the breast is known. This approach is an essential prior information for the inverse scattering problem by manipulating breast only in the analysis region. The breast model is also discretized to 6 mm resolution, so that it composed of 847 voxels. We characterized the complex permittivity of corresponding voxel with adipose tissue, fibro-glandular tissue and tumor in the form of {ε, σ} as detailed in Fig. 3.

B. Numerical Results

Numerical programs involving the implementation of the imaging sensor and characterized complex permittivity of voxels have been developed to investigate the effectiveness of double mesh scheme for image reconstruction. A single frequency of 4.5 GHz is used in all numerical simulations.

Fig. 4 shows relative permittivity (left) and conductivity (right) of the exact model and reconstruction images for breast model without fibro-glandular tissue. Here, the images are shown in the vertical cut view for clarity images of the tumor. Fig. 4(a) is the exact model in fine mesh with 847 voxels. Fig. 4(b) shows image reconstruction in coarse mesh with 108 voxels. We can observed that the image reconstruction is inadequate, and both parameters of the tumor are indistinct when compared to the exact model. Next, we employ double mesh into the red box area, as indicated in Fig. 4(b). The corresponding voxels in this area are 136 voxels, and overall yields 207 voxels in the double mesh scheme. The images shown in Fig. 4(c) are reconstructed sufficiently in double mesh, and clearly indicate the tumor presence for both parameters. The complex permittivity of tumor shown in Fig. 4(c) is {ε, σ} = {24.04, 3.45 [S/m]}

Fig. 5 shows the exact model and reconstruction images for breast model with fibro-glandular tissue presence after 400 iterations. The exact model in fine mesh with 847 voxels is shown in Fig 5(a). For coarse mesh composed of 108 voxels in Fig. 5(b), the image reconstruction in both relative permittivity and

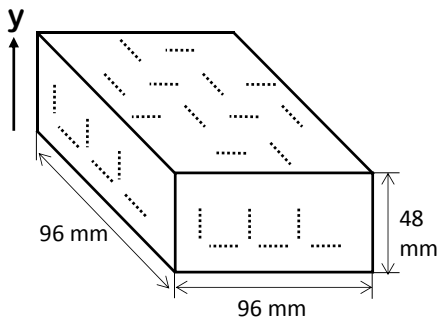

Fig. 2. Proposed imaging sensor

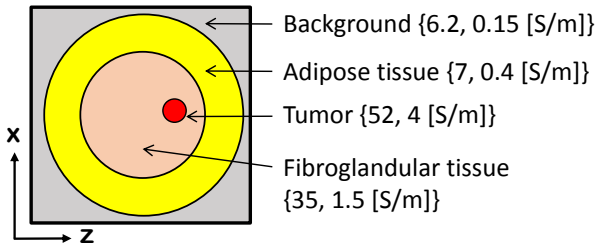

Fig. 3. A simple breast model

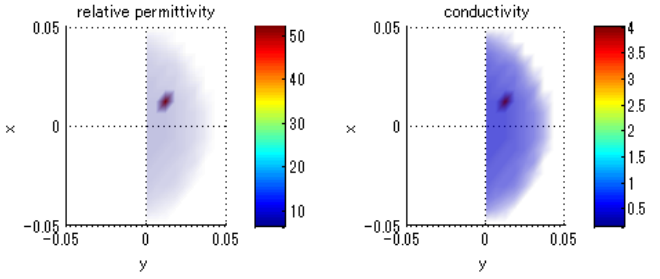

(a) Exact model in fine mesh

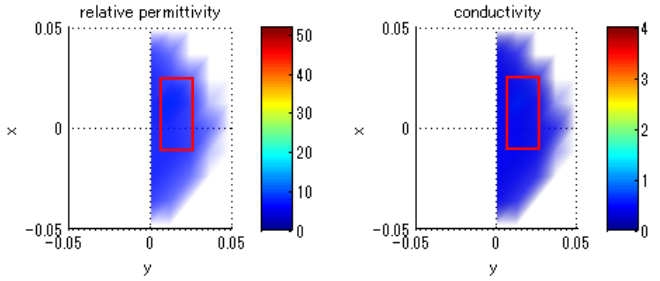

(b) Coarse mesh

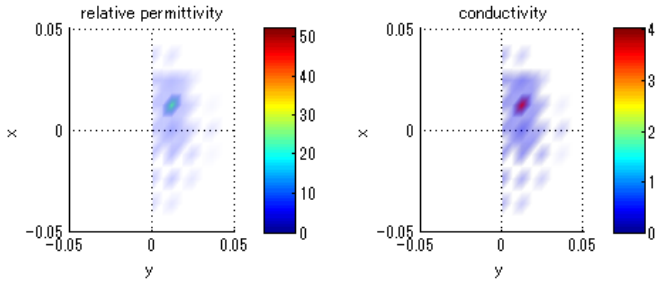

(c) Double mesh

Fig. 4. Image reconstruction of model after 100 iterations

conductivity is insufficient, and the tumor presence could not be identified. Here, similarly to model in Fig. 4, we apply double mesh into red box area as shown in Fig. 5(b). The corresponding voxels allocated in this area are 72 voxels, and overall generates 159 voxels in the double mesh scheme. We could observed that the images of the double mesh shown in Fig 5(c) are reconstructed successfully, and we managed to distinguish the tumor presence for both parameters. The complex permittivity of tumor is estimated to {ε, σ} = {51.94, 4.45 [S/m]}.

IV. Conclusion

We have confirmed the effectiveness of applying DBIM and double mesh scheme into image reconstruction algorithm employing the proposed imaging sensor and a simple breast model. In conclusion, the numerical simulation results demonstrated that the double mesh scheme is capable of reconstructing desired images and complex permittivity distribution, even small size of tumor.

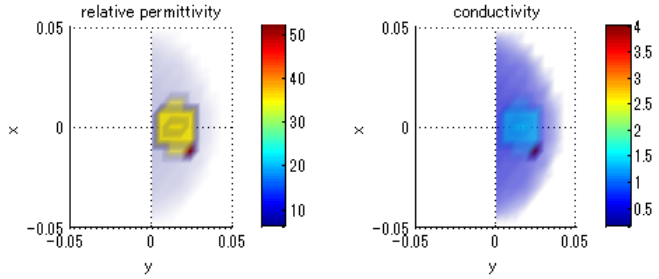

(a) Exact model in fine mesh

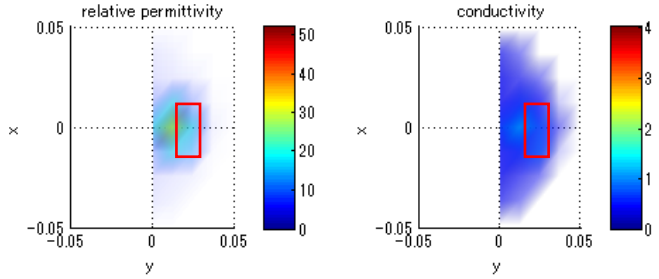

(b) Coarse mesh

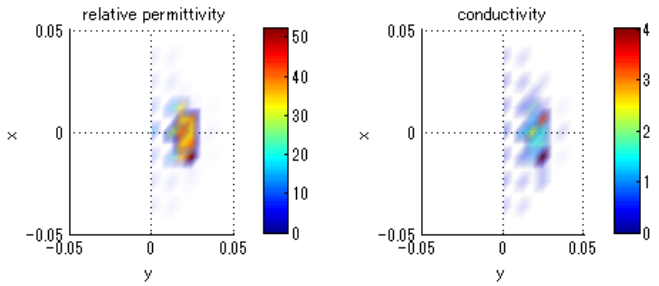

(c) Double mesh

Fig. 5. Image reconstruction of model after 400 iterations

References

[1] K. Saika, and T. Sobue, "Epidemiology of Breast Cancer in Japan and the US, " Journal of the Japan Medical Association (JMAJ), Vol. 52, No. 1, 39-44, Jan/Feb 2013.

[2] M. Lazebnik, D. Popovic, L. McCartney, C. B. Watkins, M. J. Lindstrom, J. Harter, S. Sewall, T. Ogilvie, A. Magliocco, T. M. Breslin, W. Temple, D. Mew, J. H. Booske, M. Okoniewski, and S. C. Hagness, "A large-scale study of the ultra-wideband microwave dielectric properties of normal, benign, and malignant breast tissues obtained from cancer surgeries, " Phys. Med. Biol., Vol. 52, No. 20, 6093-6115, Oct 2007.

[3] Latifah Mohamed, Yoshihiko Kuwahara, "Polarization Diversity on Microwave Tomography, " Proc. of iWAT 2014 , Mar 2014.

[4] N. Ozawa and Y. Kuwahara, "Considerations of antennas for microwave mammography, " TJMW2014, TH3-4, 2014.

[5] Latifah Mohamed, and Yoshihiko Kuwahara, "Distortion Born Iterative Method in Microwave Tomography -A Numerical Study of 3D Non-Debye and Debye Model-," Proc. of Thailand-Japan Microwave 2014, TH4-1, Nov 2014.

[6] N. Joachimowicz, C. Pichot, and J. P. Hugonin, "Inverse scattering: an iterative numerical method for electromagnetic imaging, " IEEE Trans. on Antennas and Propagation, Vol. 39, No. 12, 1742-1752, Dec 1991.

[7] J. D. Shea, P. Kosmas, V. Veen and S. C. Hagness, "Contrast-enhanced microwave imaging of breast tumors: a computational study using 3D realistic numerical phantoms, " Inverse Problem 26 074009, 2010.

[8] J. D. Shea, P. Kosmas, S. C. Hagness, and B. D. V Veen, "Three-dimensional microwave imaging of realistic numerical breast phantoms via a multiple-frequency inverse scattering technique, " Med. Phys. 37 (8), Aug 2010.

[9] Song Wang, Yukio Ueda, Huafeng Liu, "Meshfree Strategy for Diffuse Optical Tomography Image Reconstruction," in International Conference of Medical Image Analysis and Clinical Application (MIACA), pp. 87-90, 2010.

[10] Paul M. Meaney, Keith D. Paulsen, Thomas P. Ryan, "Microwave Thermal Imaging Using a Hybrid Element Method with a Dual Mesh Scheme for Reduced Computation Time," Proceedings of the 15th Annual International Conference of the IEEE Engineering in Medicine and Biology Society, pp. 96-97, 1993.

[11] Keith D. Paulsen, Paul M. Meaney, Michael J. Moskowitz, John M. Sullivan Jr, "A Dual Mesh Scheme for Finite Element Based Reconstruction Algorithms," IEEE Trans. on Medical Imaging, Vol. 14, No. 3, pp. 504-514, Sep 1991.

[12] Jae Hoon Lee, Amit Joshi, Eva M. Sevick-Muraca, "Adaptive Technique for Fluorescence Enhanced Optical Tomography using Tetrahedral Dual-mesh," 4th IEEE International Symposium on Biomedical Imaging: From Nano to Macro, pp. 1376-1379, 2007.